Three-body effects in Casimir-Polder repulsion

Kimball A. Milton, E. K. Abalo, Prachi Parashar, Nima Pourtolami, Iver Brevik, Simen Å. Ellingsen, Stefan Yoshi Buhmann, and Stefan Scheel

Phys. Rev. A **91**, 042510 — Published 28 April 2015

DOI: 10.1103/PhysRevA.91.042510

Casimir-Polder repulsion: Three-body effects

Kimball A. Milton,[1,*] E. K. Abalo,[1,†] Prachi Parashar,[1,2,‡] Nima Pourtolami,[3,§] Iver Brevik,[4,¶] Simen Å. Ellingsen,[4,**] Stefan Yoshi Buhmann,[5,††] and Stefan Scheel[6,‡‡]

[1]*Homer L. Dodge Department of Physics and Astronomy, University of Oklahoma, Norman, OK 73019-2061, USA*
[2]*Departmeht of Physics, Southern Illinois University–Carbondale, Carbondale, IL 62901 USA*
[3]*Department of Physics, Concordia University, 7141 Sherbrooke St. W., SP-367.7, Montreal, Quebec, Canada H4B 1R6*
[4]*Department of Energy and Process Engineering, Norwegian University of Science and Technology, N-7491 Trondheim, Norway*
[5]*Physikalisches Institut, Albert-Ludwigs-Universität Freiburg, Hermann-Herder-Str. 3, 79104 Freiburg, Germany and Freiburg Institute for Advanced Studies, Albert-Ludwigs-Universität Freiburg, Albertstr. 19, 79104 Freiburg, Germany*
[6]*Institut für Physik, Universität Rostock, Universitätsplatz 3, D-18051 Rostock, Germany*

In this paper we study an archetypical scenario in which repulsive Casimir-Polder forces between an atom or molecule and two macroscopic bodies can be achieved. This is an extension of previous studies of the interaction between a polarizable atom and a wedge, in which repulsion occurs if the atom is sufficiently anisotropic and close enough to the symmetry plane of the wedge. A similar repulsion occurs if such an atom passes a thin cylinder or a wire. An obvious extension is to compute the interaction between such an atom and two facing wedges, which includes as a special case the interaction of an atom with a conducting screen possessing a slit, or between two parallel wires. To this end we further extend the electromagnetic multiple-scattering formalism for three-body interactions. To test this machinery we reinvestigate the interaction of a polarizable atom between two parallel conducting plates. In that case, three-body effects are shown to be small, and are dominated by three- and four-scattering terms. The atom-wedge calculation is illustrated by an analogous scalar situation, described in the Appendix. The wedge-wedge-atom geometry is difficult to analyze because this is a scale-free problem. But it is not so hard to investigate the three-body corrections to the interaction between an anisotropic atom or nanoparticle and a pair of parallel conducting cylinders, and show that the three-body effects are very small and do not affect the Casimir-Polder repulsion at large distances between the cylinders. Finally, we consider whether such highly anisotropic atoms needed for repulsion are practically realizable. Since this appears rather difficult to accomplish, it may be more feasible to observe such effects with highly anisotropic nanoparticles.

PACS numbers: 42.50.Lc, 32.10.Dk, 12.20.-m, 03.70.+k

I. INTRODUCTION

It is quite remarkable that after nearly seven decades, interest in the so-called Casimir effect [1] remains so high. There have been many theoretical and experimental developments in the last few years. For a review of the status of quantum vacuum energy phenomena in general, the reader is referred to the volume edited by Dalvit et al. [2].

One of the hottest topics in the field is the subject of repulsive Casimir effects. This could have a major impact in nanotechnology, where at distances well below 1 μm, Casimir forces can play a dominating role. Repulsion can occur between electric and magnetic bodies, between electric bodies separated by a medium with an intermediate value of permittivity, or purely due to the geometry of the two bodies. The geometric repulsion that was demonstrated in Ref. [3] was based on numerical methods. A great deal of effort has been given to understanding the underlying analytical structure of repulsive effects [4–6]. A brief review, with references, is provided in Ref. [7]. For further work on repulsion see Refs. [8–10].

In this paper, we will further develop the multiple-scattering approach to include three-body effects, which was introduced in the scalar context in Refs. [11–13], in particular in the context of Casimir repulsion. The electromagnetic formulation is in turn based on Green's dyadics, which have a long history. The Green's dyadic approach to computing the Casimir effect was first proposed in Refs. [14, 15]. This was a tensorial generalization of the scalar Green's function variational approach Schwinger had given a few years earlier [16]. All of this was in the direct line of evolution to what is now referred to as the multiple scattering method.

Although it is well-appreciated that Casimir forces

*Electronic address: milton@nhn.ou.edu
†Electronic address: ekabalo@gmail.com
‡Electronic address: prachi@nhn.ou.edu
§Electronic address: nima.pourtolami@gmail.com
¶Electronic address: iver.h.brevik@ntnu.no
**Electronic address: simen.a.ellingsen@ntnu.no
††Electronic address: stefan.buhmann@physik.uni-freiburg.de
‡‡Electronic address: stefan.scheel@uni-rostock.de

are not additive, most work on such interactions has concentrated on forces between two bodies. But the multiple-scattering formalism is easily generalized to include three-body interactions. In Sec. II of this paper we develop the three-body formalism for the electromagnetic case. This is relevant to computing the force between a polarizable atom and two co-planar half planes, forming a slit, for example. As a simple illustration of the formalism, we re-examine, in Sec. III, the interaction between an atom and two parallel conducting plates, first considered by Barton [17]. Naturally, the two-body forces dominate when the atom is near one or the other of the plates, and three-body effects become significant at the several percent level only when the atom is roughly equidistant from the two plates, but then the force is quite small. In Ref. [18] we examined the nonmonotonicity that can arise when two polarizable atoms are near each other and close to a conducting plate. These are reminiscent of effects seen between two macroscopic objects and a wall [19, 20]; our work generalized that given in Ref. [21]. We broke up the three-body terms into three- and four-scattering contributions; although both are comparable at short distances, as expected, the former dominate for atoms far from the plate. In order to work out the three-body effects for an atom interacting with two half-planes, constituting a slit in a conducting plane, or more generally, facing wedges, in Sec. IV A we work out the scattering matrix for a single wedge, and then, in Sec. IV B, apply that to recalculate the two-body repulsion found in Ref. [4]. Because of the complexity of the calculation, a scalar analog is also considered in the Appendix. We then go on to consider three-body effects between a polarizable atom and a pair of parallel conducting cylinders in Sec. V. In Ref. [5] we showed that for an anisotropic atom moving along a line perpendicular to but not intersecting a perfectly conducting cylinder, and polarizable along that same line, a repulsive force occurs near the cylinder, provided the distance of closest approach is sufficiently large compared to the radius of the cylinder. (The same does not occur for a sphere.) Here we consider the three-body effects due to a second cylinder parallel to the first, so the pair forms an aperture, perpendicular to which the anisotropic atom moves. We adapt our formalism to this case, where a multipole expansion is also possible, and show that when the distance between the cylinders is sufficiently large, repulsion is not affected by the three-body corrections, since the latter are very small. Finally, in Sec. VI, we present a calculation that suggests that highly anisotropic atoms, necessary to exhibit the repulsive effects we are considering, may be beyond reach. Therefore, as in the numerical calculations of Ref. [3], it may be more appropriate to consider the interaction with highly anisotropic conducting nanoparticles, such as needles, as suggested in related work on negative Casimir-Polder entropy [22].

II. THREE-BODY CASIMIR ENERGY

The multiple scattering formulation has proved exceptionally useful in computing Casimir energies for complex configurations. It is usually presented in terms of potentials, where the potential stands in for the deviation of the permittivity from its vacuum value, for instance. Here, however, we wish from the outset to consider perfect conductors, so we give the formulation entirely in terms of scattering matrices. In particular, we wish to analyze three-body effects. The formalism we apply here appears in many places; recent examples are Refs. [22, 23]. We use natural units, with $\hbar = c = 1$, and Heaviside-Lorentz electromagnetic units, except for the definition of the polarizability.

The quantum vacuum energy, with the bulk vacuum energy subtracted, is in general given by

$$E = \frac{i}{2}\,\mathrm{Tr}\ln \boldsymbol{\Gamma}\boldsymbol{\Gamma}_0^{-1}, \tag{2.1}$$

where the Tr symbol represents a trace over tensor indices as well as spatial coordinates. Here $\boldsymbol{\Gamma}_0$ is the free Green's dyadic, which, for a given frequency ω, can be written as

$$\boldsymbol{\Gamma}_0(\mathbf{r},\mathbf{r}') = (\mathbf{1}\omega^2 + \boldsymbol{\nabla}\boldsymbol{\nabla})G_0(|\mathbf{r}-\mathbf{r}'), \tag{2.2}$$

in terms of the free Helmholtz Green's function

$$G_0(R) = \frac{e^{i|\omega|R}}{4\pi R}, \quad R = |\mathbf{r}-\mathbf{r}'|. \tag{2.3}$$

The full Green's dyadic $\boldsymbol{\Gamma}$ satisfies the same differential equation as the free Green's dyadic,

$$\boldsymbol{\Gamma}_0^{-1}\boldsymbol{\Gamma} = \mathbf{1}, \tag{2.4}$$

where

$$\boldsymbol{\Gamma}_0^{-1} = \frac{1}{\omega^2}\boldsymbol{\nabla}\times\boldsymbol{\nabla}\times -\mathbf{1} = \frac{1}{\omega^2}\left[\boldsymbol{\nabla}\boldsymbol{\nabla} - (\nabla^2+\omega^2)\mathbf{1}\right]. \tag{2.5}$$

Here we have adopted a matrix notation for both the tensor indices and the spatial coordinates, so

$$\mathbf{1} = \mathbf{1}\delta(\mathbf{r}-\mathbf{r}'), \tag{2.6}$$

where on the right $\mathbf{1}$ refers to the tensor indices only. The conducting surfaces S appear through boundary conditions on the Green's dyadic,

$$\hat{\mathbf{n}}\times\boldsymbol{\Gamma}\Big|_S = 0, \tag{2.7}$$

where $\hat{\mathbf{n}}$ is the outward normal to the surface at the point in question. We may define the scattering matrix $\mathbf{T}$ by

$$\boldsymbol{\Gamma} = \boldsymbol{\Gamma}_0 + \boldsymbol{\Gamma}_0\mathbf{T}\boldsymbol{\Gamma}_0, \tag{2.8}$$

so that

$$\mathbf{T} = -\boldsymbol{\Gamma}_0^{-1} + \boldsymbol{\Gamma}_0^{-1}\boldsymbol{\Gamma}\boldsymbol{\Gamma}_0^{-1}. \tag{2.9}$$

Now we turn to the quantum interaction of three bodies. It seems easiest to start with the situation where the bodies may be described by potentials $\mathbf{V}_i$, $i = 1, 2, 3$, and then write the result in a form in which only the $\mathbf{T}$ operators appear, so it applies to the conducting boundary problem, defined by Eq. (2.7). The total potential is $\mathbf{V} = \mathbf{V}_1 + \mathbf{V}_2 + \mathbf{V}_3$, and the vacuum energy is given by the trace-log of

$$\mathbf{\Gamma}\mathbf{\Gamma}_0^{-1} = (\mathbf{1} - \mathbf{\Gamma}_0\mathbf{V})^{-1}, \tag{2.10}$$

or

$$E = -\frac{i}{2}\,\mathrm{Tr}\ln(\mathbf{1} - \mathbf{\Gamma}_0\mathbf{V}). \tag{2.11}$$

Now it is easy to see that

$$\begin{aligned} 1 - \mathbf{\Gamma}_0(\mathbf{V}_1 + \mathbf{V}_2 + \mathbf{V}_3) &= (\mathbf{1} - \mathbf{\Gamma}_0\mathbf{V}_1 - \mathbf{\Gamma}_0\mathbf{V}_2) \\ &\times \left[\mathbf{1} - (\mathbf{1} - \mathbf{\Gamma}_1\mathbf{V}_2)^{-1}\mathbf{\Gamma}_1\mathbf{V}_2\mathbf{\Gamma}_1\mathbf{V}_3(\mathbf{1} - \mathbf{\Gamma}_1\mathbf{V}_3)^{-1}\right] \\ &\times(\mathbf{1} - \mathbf{\Gamma}_0\mathbf{V}_1)^{-1}(\mathbf{1} - \mathbf{\Gamma}_0\mathbf{V}_1 - \mathbf{\Gamma}_0\mathbf{V}_3). \end{aligned} \tag{2.12}$$

Here we have introduced the Green's dyadic belonging to potential i alone,

$$\mathbf{\Gamma}_i = (\mathbf{1} - \mathbf{\Gamma}_0\mathbf{V}_i)^{-1}\mathbf{\Gamma}_0. \tag{2.13}$$

Now in Eq. (2.12) the factors before and after the square brackets refer to only one- and two-body interactions (the latter referring to interactions between bodies 1 and 2, and 1 and 3, respectively), so the two-body interactions between 2 and 3, and three-body interactions are all contained in the quantity in square brackets. Now, in terms of the potential, the corresponding scattering matrix is

$$\mathbf{T}_i = \mathbf{V}_i(\mathbf{1} - \mathbf{\Gamma}_0\mathbf{V}_i)^{-1}. \tag{2.14}$$

Introducing the modified scattering matrix defined by Shajesh and Schaden [13],

$$\tilde{\mathbf{T}} = \mathbf{T}\mathbf{\Gamma}_0, \tag{2.15}$$

and using the cyclic property of the trace, we find the two and three body terms:

$$E_{23} = -\frac{i}{2}\,\mathrm{Tr}\ln(\mathbf{1} - \tilde{\mathbf{T}}_2\tilde{\mathbf{T}}_3), \tag{2.16}$$

which is sometimes called the $TGTG$ formula, and

$$\begin{aligned} E_{123} = -\frac{i}{2}\,\mathrm{Tr}\ln\Bigg(\mathbf{1} - \mathbf{X}_{23}\Big[&\mathbf{X}_{21}\tilde{\mathbf{T}}_2(\mathbf{1} + \tilde{\mathbf{T}}_1)\mathbf{X}_{31} \\ &\times\tilde{\mathbf{T}}_3(\mathbf{1} + \tilde{\mathbf{T}}_1) - \tilde{\mathbf{T}}_2\tilde{\mathbf{T}}_3\Big]\Bigg), \end{aligned} \tag{2.17}$$

where

$$\mathbf{X}_{ij} = (\mathbf{1} - \tilde{\mathbf{T}}_i\tilde{\mathbf{T}}_j)^{-1}. \tag{2.18}$$

Expression (2.17) has a rather evident geometrical interpretation in terms of multiple scattering off the three objects. This is not written in as symmetrical a form as in Ref. [13], but is somewhat simpler, particular for the Casimir-Polder applications that follow, where body 1 represents the atom, so is treated weakly.

III. POLARIZABLE ATOMS BETWEEN PARALLEL CONDUCTING PLATES

As a simple check of the machinery developed in the previous section, we revisit the calculation of the interaction energy of an anisotropically polarizable atom between parallel conducting plates, a geometry first analyzed by Barton [17]. Since we know the Green's dyadic $\mathbf{\Gamma}$ for parallel plates, it is easy to derive the interaction energy from the general Casimir-Polder formula

$$E_{CP} = -\int_{-\infty}^{\infty} d\zeta\,\mathrm{Tr}\,\boldsymbol{\alpha}\cdot\mathbf{\Gamma}, \tag{3.1}$$

where the integration is over imaginary frequency, $\omega \to i\zeta$.[1] Here the (in general, anisotropic) polarizability of the atom is $\boldsymbol{\alpha}$. In the following we will assume $\boldsymbol{\alpha}$ is independent of frequency, i.e., we are working in the static approximation. The interaction energy for one conducting plate at $z = 0$, one at $z = a$, and the atom at $z = Z$, $0 < Z < a$, is

$$\begin{aligned} E_{CP} = \frac{\alpha_{11} + \alpha_{22} - \alpha_{33}}{4\pi a^4}\zeta(4) \\ - \frac{\mathrm{tr}\,\boldsymbol{\alpha}}{8\pi a^4}\left[\zeta(4, Z/a) + \zeta(4, 1 - Z/a)\right], \end{aligned} \tag{3.2}$$

in terms of the Hurwitz zeta function.[2] Here the two-body interactions between the atom and one or the other plate are isolated by extracting the parts singular as $Z \to 0$ or $Z \to a$:

$$\begin{aligned} \zeta(4, Z/a) &= \left(\frac{a}{Z}\right)^4 + \zeta(4, 1 + Z/a), \\ \zeta(4, 1 - Z/a) &= \left(\frac{a}{a - Z}\right)^4 + \zeta(4, 2 - Z/a). \end{aligned} \tag{3.3}$$

The total Casimir-Polder energy is the sum of two-body and three-body terms,

$$E_{CP} = E_{12} + E_{13} + E_{123}, \tag{3.4}$$

where 1 denotes the atom, 2 the lower plate, and 3 the upper plate. Here

$$E_{12} = -\frac{\mathrm{tr}\,\boldsymbol{\alpha}}{8\pi Z^4}, \quad E_{13} = -\frac{\mathrm{tr}\,\boldsymbol{\alpha}}{8\pi(a - Z)^4}, \tag{3.5a}$$

---

[1] This replacement requires knowledge of the analytic properties of the integrand. There can be serious subtleties involved in this "Euclidean transformation," for example, see Ref. [24]. See also Ref. [25].

[2] The particular combinations of Hurwitz zeta functions occurring here and in the following are striking. Such combinations occur in several places, for instance when considering the Casimir energy for two parallel plates in D dimensional spacetimes, where the argument 4 is replaced by D. Two of the first papers in this direction are Refs. [26, 27]. See also Ref. [28]. Related structures appear for the theory of the piecewise uniform string [29–31].

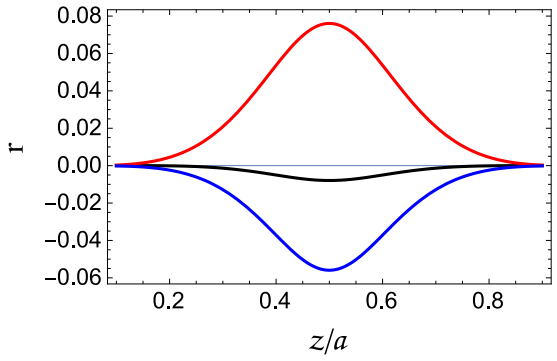

FIG. 1: (Color online) Three-body contributions to the Casimir-Polder interaction of an anisotropically polarizable atom between two parallel polarizable plates. What is plotted is the ratio of the three-body contribution relative to the total energy, $r = E_{123}/E_{CP}$. The three-body contributions are generally very small. They become appreciable only far from both plates, where the Casimir-Polder energy is very small. Plotted is the ratio for isotropic atoms (middle curve), atoms polarizable only in the direction perpendicular to the plates (top curve), and polarizable only parallel to the plates (bottom curve). In the case when only $\alpha_{zz} \neq 0$, the sign of the three-body correction is the same as that of the two-body term.

and

$$E_{123} = \frac{\alpha_{11}+\alpha_{22}-\alpha_{33}}{4\pi a^4}\zeta(4) - \frac{\operatorname{tr}\boldsymbol{\alpha}}{8\pi a^4}\left[\zeta(4,1+Z/a)+\zeta(4,2-Z/a)\right]. \tag{3.5b}$$

Note that the first term in E_{123} is independent of Z, so it does not contribute to the Casimir-Polder force on the atom, but is a Casimir-Polder correction to the Casimir force between the plates. The two-body energies overwhelmingly dominate the Casimir-Polder interaction, as shown in Fig. 1. For isotropic atoms, the largest three body correction is only a 0.8% reduction at the midpoint between the plates, where the energy is very small. For atoms only polarizable parallel to the z direction the three-body correction is an 8% increase at the place where the energy is the smallest, while for purely transversely polarizable atoms, the three-body correction is a 6% reduction at the midpoint.

A. Multiple-scattering calculation

Since in more general situations we do not have an exact solution available, we want to calculate the three-body corrections (3.5b), using the multiple-scattering formula (2.17). For this purpose, we need to compute the scattering operators for the three bodies.

The scattering matrix for the atom is simply

$$\mathbf{T}_1(\mathbf{r},\mathbf{r}') = \mathbf{V}_1(\mathbf{r},\mathbf{r}') = 4\pi\boldsymbol{\alpha}\delta(\mathbf{r}-\mathbf{R})\delta(\mathbf{r}-\mathbf{r}'), \tag{3.6}$$

where $\mathbf{R} = (0,0,Z)$ is the position of the atom. The free electromagnetic Green's dyadic can be written as

$$\boldsymbol{\Gamma}_0(\mathbf{r}-\mathbf{r}') = \int \frac{(d\mathbf{k}_\perp)}{(2\pi)^2} e^{i\mathbf{k}_\perp\cdot(\mathbf{r}-\mathbf{r}')_\perp}\boldsymbol{\gamma}_0(z,z'), \tag{3.7}$$

where

$$\boldsymbol{\gamma}_0(z,z') = (\mathbf{E}+\mathbf{H})\frac{1}{2\kappa}e^{-\kappa|z-z'|}, \tag{3.8}$$

with the usual abbreviation $\kappa = \sqrt{k^2+\zeta^2}$. Here $\mathbf{E}$ and $\mathbf{H}$ are matrices corresponding to the transverse electric (TE) and transverse magnetic (TM) modes,

$$\mathbf{E} = -\zeta^2\begin{pmatrix} s^2 & -cs & 0 \\ -cs & c^2 & 0 \\ 0 & 0 & 0 \end{pmatrix},$$
$$\mathbf{H}(z,z') = \begin{pmatrix} c^2\partial_z\partial_{z'} & cs\partial_z\partial_{z'} & ikc\partial_z \\ cs\partial_z\partial_{z'} & s^2\partial_z\partial_{z'} & iks\partial_z \\ -ikc\partial_{z'} & -iks\partial_{z'} & k^2 \end{pmatrix}. \tag{3.9}$$

Here $k^2 = \mathbf{k}_\perp^2$ and c (s) is the cosine (sine) of the angle between the direction of $\mathbf{k}_\perp$ and the x-axis, $c = k_x/k$, $s = k_y/k$. The polarization operators are transverse, in the sense that

$$i\mathbf{k}_\perp\cdot\mathbf{H} + \partial_z\hat{\mathbf{z}}\cdot\mathbf{H} = 0, \tag{3.10}$$

and similarly for $\mathbf{E}$. Thus the modified scattering matrix for the atom is

$$\tilde{\mathbf{T}}_1(\mathbf{r},\mathbf{r}') = 4\pi\boldsymbol{\alpha}\delta(z-Z)\delta(\mathbf{r}_\perp)\int\frac{(d\mathbf{k}_\perp)}{(2\pi)^2}e^{i\mathbf{k}_\perp\cdot(\mathbf{r}-\mathbf{r}')_\perp} \times(\mathbf{E}+\mathbf{H})(z,z')\frac{1}{2\kappa}e^{-\kappa|z-z'|}. \tag{3.11}$$

The following composition properties of the $\mathbf{E}$ and $\mathbf{H}$ operators are easily checked:

$$\mathbf{EH} = 0, \tag{3.12a}$$
$$\mathbf{EE} = -\zeta^2\mathbf{E}, \tag{3.12b}$$
$$\mathbf{H}(z,z')\mathbf{H}(z'',z''') = (k^2+\partial_{z'}\partial_{z''})\mathbf{H}(z,z'''). \tag{3.12c}$$

For a single plate, say a conducting plate 2 at $z = 0$, we have the reduced Green's dyadic in the form

$$\boldsymbol{\gamma} = \mathbf{E}g^E + \mathbf{H}g^H, \tag{3.13}$$

where

$$g^{E,H}(z,z') = g_0(z,z') \mp \frac{1}{2\kappa}e^{-\kappa(|z|+|z'|)}\begin{cases}1,\\ \operatorname{sgn}(z)\operatorname{sgn}(z'),\end{cases}$$
$$g_0(z,z') = \frac{1}{2\kappa}e^{-\kappa|z-z'|}. \tag{3.14}$$

Then the reduced modified scattering matrix is

$$\tilde{\mathbf{t}}_2(z,z') = \boldsymbol{\gamma}_0^{-1}(\boldsymbol{\gamma}-\boldsymbol{\gamma}_0)(z,z'). \tag{3.15}$$

This is evaluated by using the transverse property of $\mathbf{E}$ and $\mathbf{H}$ [hence, the vector Helmholtz operator reduces to $-\nabla^2+\zeta^2$—see Eq. (2.5)] and

$$\left(-\frac{d^2}{dz^2}+\kappa^2\right)e^{-\kappa|z|} = 2\kappa\delta(z), \tag{3.16a}$$

$$\left(-\frac{d^2}{dz^2}+\kappa^2\right)\mathrm{sgn}(z)e^{-\kappa|z|} = 2\delta'(z)e^{-\kappa|z|}. \tag{3.16b}$$

Thus the modified scattering matrix for a conducting plate at $z=0$ is

$$\tilde{\mathbf{t}}_2(z,z') = \frac{1}{\zeta^2}\Big[\mathbf{E}(z,z')\delta(z)e^{-\kappa|z'|} + \mathbf{H}(z,z')\frac{1}{\kappa}\delta'(z)e^{-\kappa|z|}\mathrm{sgn}(z')e^{-\kappa|z'|}\Big]. \tag{3.17}$$

However, because $\delta'(z)$ is an instruction to integrate by parts and evaluate at $z=0$, which action is on the exponential propagators occurring in every case, we can use, as in Ref. [22],

$$\tilde{\mathbf{t}}_2(z,z') = \frac{1}{\zeta^2}(\mathbf{E}-\mathbf{H})(z,z')\delta(z)e^{-\kappa|z'|}. \tag{3.18}$$

Then it is easy to see that the two-body interaction energy between the atom and the plate is as expected:

$$E_{12} = \frac{i}{2}\,\mathrm{Tr}\,\tilde{\mathbf{T}}_1\tilde{\mathbf{T}}_2 = -\frac{\mathrm{tr}\,\boldsymbol{\alpha}}{8\pi Z^4}. \tag{3.19}$$

B. CP interaction between atom and two parallel conducting plates

The three-body interaction is worked out by simplifying the multiple-scattering formula (2.17) for the case when there is only one interaction with the atom, since that coupling is always weak:

$$E_{123} = \frac{i}{2}\,\mathrm{Tr}\,\mathbf{X}_{23}\big(\tilde{\mathbf{T}}_2\tilde{\mathbf{T}}_1\tilde{\mathbf{T}}_2\tilde{\mathbf{T}}_3+\tilde{\mathbf{T}}_2\tilde{\mathbf{T}}_3\tilde{\mathbf{T}}_1\tilde{\mathbf{T}}_3 + \tilde{\mathbf{T}}_2\tilde{\mathbf{T}}_1\tilde{\mathbf{T}}_3+\tilde{\mathbf{T}}_2\tilde{\mathbf{T}}_3\tilde{\mathbf{T}}_1\big), \tag{3.20}$$

where the $\tilde{\mathbf{T}}$ operators are given in Sec. III A.

Let us look at the $\mathbf{E}$ and $\mathbf{H}$ parts separately. For the TE part,

$$\mathbf{X}_{23}\mathbf{E} = \mathbf{E}\frac{1}{1-e^{-2\kappa a}}\delta(z), \tag{3.21}$$

so

$$E_{123}^{\mathrm{TE}} = \frac{1}{4\pi^2}\int d\zeta\,(d\mathbf{k}_\perp)\,\mathrm{tr}\,\boldsymbol{\alpha}\left(-\frac{\mathbf{E}}{\zeta^2}\right)\frac{e^{-2\kappa a}}{1-e^{-2\kappa a}}\left(-\frac{\zeta^2}{2\kappa}\right) \times\left[e^{-2\kappa Z}+e^{-2\kappa(a-Z)}-2\right], \tag{3.22}$$

where integrating over the directions of $\mathbf{k}_\perp$ gives for the trace

$$\mathrm{tr}\,\boldsymbol{\alpha}\left(-\frac{\mathbf{E}}{\zeta^2}\right)\to\frac{1}{2}(\alpha_{11}+\alpha_{22}). \tag{3.23}$$

Thus the TE contribution is

$$\begin{aligned}E_{123}^{\mathrm{TE}} &= -\frac{\alpha_{11}+\alpha_{22}}{12\pi}\int_0^\infty d\kappa\,\kappa^3\frac{1}{e^{2\kappa a}-1} \times\left[-2+e^{-2\kappa Z}+e^{-2\kappa(a-Z)}\right]\\ &= -\frac{\alpha_{11}+\alpha_{22}}{32\pi a^4}\Big[-2\zeta(4)+\zeta(4,1+Z/a) +\zeta(4,2-Z/a)\Big].\end{aligned} \tag{3.24}$$

The TM contribution is similarly worked out, with the result

$$\begin{aligned}E_{123}^{\mathrm{TM}} &= -\frac{1}{2\pi}\int_0^\infty\frac{d\kappa\,\kappa^3}{e^{2\kappa a}-1}\Big\{\frac{\alpha_{11}+\alpha_{22}}{2} \times\left[e^{-2\kappa Z}+e^{2\kappa(a-Z)}-2\right]\\ &\qquad+\frac{2}{3}\alpha_{33}\left[e^{-2\kappa Z}+e^{-2\kappa(a-Z)}+2\right]\Big\}\\ &= -\frac{3(\alpha_{11}+\alpha_{22})}{32\pi a^4} \times[-2\zeta(4)+\zeta(4,1+Z/a)+\zeta(4,2-Z/a)]\\ &\quad-\frac{\alpha_{33}}{8\pi a^4}\left[2\zeta(4)+\zeta(4,1+Z/a)+\zeta(4,2-Z/a)\right].\end{aligned} \tag{3.25}$$

Adding this to the TE contribution (3.24), gives the three-body energy (3.5b).

The three-body corrections are dominated by the three- and four-scattering contributions, given by the explicit scattering terms in Eq. (3.20), with the multiple-reflection quantity $\mathbf{X}_{23}$ set equal to 1. That translates into replacing the zeta functions in Eq. (3.5b) by their leading terms, $\zeta(4)\to 1$, $\zeta(4,x)\to 1/x^4$. Figure 2 compares the exact three-body corrections to the leading three- and four-scattering approximations. (It is geometrically obvious why the odd-scattering terms give contributions which are independent of the position of the atom, because the path length is then an integer multiple of the plate separation.)

IV. CASIMIR-POLDER INTERACTION BETWEEN ATOM AND WEDGE

Our goal had been to compute the three-body corrections for an atom near an aperture created by two facing wedges, as shown in Fig. 3. Here we have two parallel conducting wedges, with opening angles β, whose apexes are separated by a distance $2X$. As both interior wedge

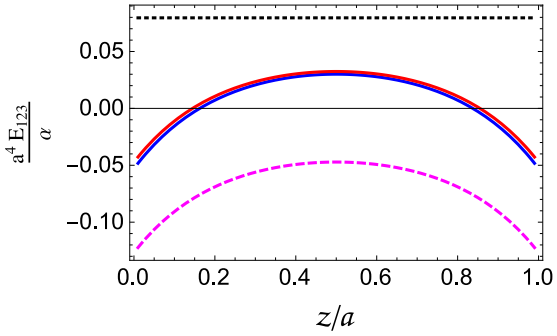

FIG. 2: (Color online) Three-body contribution to the Casimir-Polder interaction of an isotropically polarizabable atom between two parallel polarizable plates. The interaction energy is given in units of α/a^4. The upper dotted horizontal line is the three-scattering approximation, the lower dashed curve is the four-scattering approximation, the upper solid (red) curve is the sum of these two contributions, which is only slightly above the the full three-body energy (solid blue curve).

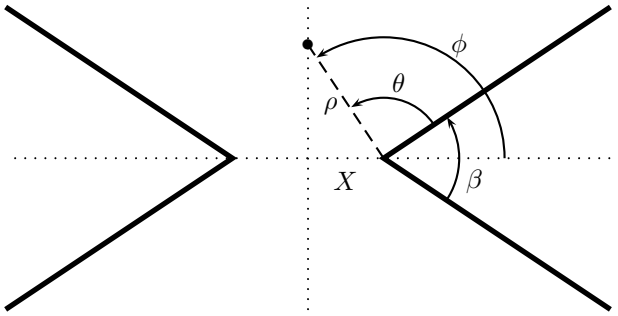

FIG. 3: Two facing conducting wedges, with an anisotropically polarizable atom passing along a line perpendicular to the symmetry plane of the wedges.

angles go to zero, the situation reduces to two conducting half-planes, lying in the same plane, with a gap between them. The Casimir-Polder interaction between the two wedges and an anisotropically polarizable molecule, located at coordinates ρ, ϕ relative to the apex of one wedge, is to be computed. In particular, we wish to study the three-body interaction, which involves scattering off all three objects, as a correction to the more elementary calculation of the interaction between the atom and a single wedge, which is given in Ref. [4]. For the latter, repulsion can be achieved for the angle ϕ sufficiently close to π, provided β is smaller than $108^\circ = 1.88$ radians.

A. Scattering Matrix for a Perfectly Conducting Wedge

In Ref. [4] we gave the Green's dyadic for a single perfectly conducting wedge, in terms of polar coordinates based at a point on the apex of the wedge. We write this most conveniently in terms of the quantity $\kappa = \sqrt{k^2+\zeta^2}$, where $\zeta = -i\omega$ is the imaginary frequency and the wavenumber in the longitudinal direction or z direction, the direction perpendicular to the plane of the figure, is k. With θ defined as the angle from the top surface of the wedge, that Green's dyadic is (the prime on the summation sign is an instruction to count the $m = 0$ term with half weight)

$$\begin{aligned}\mathbf{\Gamma}(\mathbf{r},\mathbf{r}') = \frac{2p}{\pi}{\sum_{m=0}^{\infty}}' \int_{-\infty}^{\infty}\frac{dk}{2\pi} \\ \times\Big[\mathbf{E}(\mathbf{r},\mathbf{r}')\cos mp\theta\cos mp\theta' \\ + \mathbf{H}(\mathbf{r},\mathbf{r}')\sin mp\theta\sin mp\theta'\Big]e^{ik(z-z')} \\ \times\frac{I_{mp}(\kappa\rho_<)K_{mp}(\kappa\rho_>)}{-\kappa^2}. \qquad (4.1)\end{aligned}$$

Here $\rho_>$ ($\rho_<$) is the greater (lesser) of ρ, ρ', and $p = \pi/(2\pi-\beta)$. The electric and magnetic polarization dyadic operators are

$$\begin{aligned}\mathbf{E}(\mathbf{r},\mathbf{r}') &= -\left(\hat{\boldsymbol{\rho}}\frac{1}{\rho}\partial_\theta - \hat{\boldsymbol{\theta}}\partial_\rho\right)\left(\hat{\boldsymbol{\rho}}'\frac{1}{\rho'}\partial_{\theta'} - \hat{\boldsymbol{\theta}}'\partial_{\rho'}\right) \\ &\quad\times(\nabla_\perp^2 - k^2) \\ &= -\zeta^2(\hat{\mathbf{z}}\times\boldsymbol{\nabla}_\perp)(\hat{\mathbf{z}}\times\boldsymbol{\nabla}'_\perp) \\ &= -\nabla^2(\hat{\mathbf{z}}\times\boldsymbol{\nabla}_\perp)(\hat{\mathbf{z}}\times\boldsymbol{\nabla}'_\perp), \qquad (4.2a) \\ \mathbf{H}(\mathbf{r},\mathbf{r}') &= \left[ik\left(\hat{\boldsymbol{\rho}}\partial_\rho + \hat{\boldsymbol{\theta}}\frac{1}{\rho}\partial_\theta\right) - \hat{\mathbf{z}}\nabla_\perp^2\right] \\ &\quad\times\left[-ik\left(\hat{\boldsymbol{\rho}}'\partial_{\rho'} + \hat{\boldsymbol{\theta}}'\frac{1}{\rho'}\partial_{\theta'}\right) - \hat{\mathbf{z}}\nabla_\perp'^2\right] \\ &= \left(ik\boldsymbol{\nabla}_\perp - \hat{\mathbf{z}}\kappa^2\right)\left(-ik\boldsymbol{\nabla}'_\perp - \hat{\mathbf{z}}\kappa^2\right) \\ &= [\boldsymbol{\nabla}\times(\boldsymbol{\nabla}\times\hat{\mathbf{z}})][\boldsymbol{\nabla}'\times(\boldsymbol{\nabla}'\times\hat{\mathbf{z}})]. \qquad (4.2b)\end{aligned}$$

[Here the polarization operators differ from those given previously in Eq (3.9) by the replacements $\mathbf{E}\to-\nabla_\perp^2\mathbf{E}$, $\mathbf{H}\to-\nabla_\perp^2\mathbf{H}$. For a further discussion of the properties of the polarization operators, see Ref. [23].] In the second forms in Eq. (4.2) we have used the modified Bessel equation, that is, that for either modified Bessel function

$$(-\nabla_\perp^2+\kappa^2)e^{i\nu(\theta-\theta')}\begin{Bmatrix} I_\nu(\kappa\rho) \\ K_\nu(\kappa\rho)\end{Bmatrix} = 0. \qquad (4.3)$$

In the following we will need the composition properties of these operators, analogous to those in Eq. (3.12):

$$\begin{aligned}\mathbf{E}(\mathbf{r},\mathbf{r}')\mathbf{H}(\mathbf{r}'',\mathbf{r}''') &= \mathbf{H}(\mathbf{r},\mathbf{r}')\mathbf{E}(\mathbf{r}'',\mathbf{r}''') = 0. \qquad (4.4a) \\ \mathbf{E}(\mathbf{r},\mathbf{r}')\mathbf{E}(\mathbf{r}'',\mathbf{r}''') &= \mathbf{E}(\mathbf{r},\mathbf{r}''')\nabla_\perp'^2(\nabla_\perp''^2 - k^2) \\ &\to \kappa^2\zeta^2\mathbf{E}(\mathbf{r},\mathbf{r}'''), \qquad (4.4b) \\ \mathbf{H}(\mathbf{r},\mathbf{r}')\mathbf{H}(\mathbf{r}'',\mathbf{r}''') &= \mathbf{H}(\mathbf{r},\mathbf{r}''')\nabla_\perp'^2(\nabla_\perp''^2 - k^2) \\ &\to \kappa^2\zeta^2\mathbf{H}(\mathbf{r},\mathbf{r}'''), \qquad (4.4c)\end{aligned}$$

where we will understand that after differentiation, the intermediate coordinates $\mathbf{r}'$ and $\mathbf{r}''$ are set equal and integrated over; that is, a spatial matrix multiplication is understood.

To construct the modified scattering matrices, we need the free Green's dyadic, which we can write as Eq. (2.2), where a representation for the scalar Helmholtz Green's function in cylindrical coordinates is

$$G_0(\mathbf{r}-\mathbf{r}') = \int_{-\infty}^{\infty}\frac{dk}{2\pi}e^{ik(z-z')}\frac{1}{2\pi}\sum_{m=-\infty}^{\infty}e^{im(\theta-\theta')} \times I_m(\kappa\rho_<)K_m(\kappa\rho_>). \tag{4.5}$$

It is easy to verify that in terms of the mode operators,

$$\mathbf{\Gamma}_0(\mathbf{r},\mathbf{r}') = -\frac{1}{\nabla_\perp^2}(\mathbf{E}+\mathbf{H})(\mathbf{r},\mathbf{r}')G_0(\mathbf{r}-\mathbf{r}'). \tag{4.6}$$

Using the above, we find the modified scattering matrix for the atom to be

$$\tilde{\mathbf{T}}_{\rm atom}(\mathbf{r},\mathbf{r}') = 4\pi\boldsymbol{\alpha}\delta(\mathbf{r}-\mathbf{R})(\mathbf{E}+\mathbf{H})(\mathbf{r},\mathbf{r}')\int\frac{dk}{2\pi}e^{ik(z-z')} \times\frac{1}{2\pi}\sum_{m=-\infty}^{\infty}e^{im(\theta-\theta')}\frac{I_m(\kappa\rho_<)K_m(\kappa\rho_>)}{-\kappa^2}. \tag{4.7}$$

To work out the $\tilde{\mathbf{T}}$ matrix for the wedge, we start from Eq. (2.9),

$$\tilde{\mathbf{T}} = \mathbf{\Gamma}_0^{-1}(\mathbf{\Gamma}-\mathbf{\Gamma}_0). \tag{4.8}$$

The inverse free Green's function is the differential operator given in Eq. (2.5). It is easy to check that

$$\mathbf{\Gamma}_0^{-1}\mathbf{E} = \mathbf{E}\frac{\kappa^2-\nabla_\perp^2}{\omega^2}, \tag{4.9a}$$

$$\mathbf{\Gamma}_0^{-1}\mathbf{H} = \mathbf{H}\frac{\kappa^2-\nabla_\perp^2}{\omega^2}. \tag{4.9b}$$

The Helmholtz operator appearing as the last factor here would annihilate the scalar Green's functions appearing in Eq. (4.1), except on the boundaries, where the normal derivatives give contributions to the scattering matrix that live entirely on the surface of the wedge. This is precisely the same as what occurred for the planes in Sec. III A: see Eq. (3.16). Here, because we are considering the region exterior to the wedge, we interpret the angular mode functions as follows: ($\theta\in[0,\Omega]$)

$$\cos mp\theta \to \cos mp\theta\,\eta(\theta)\,\eta(\Omega-\theta), \tag{4.10a}$$

$$\sin mp\theta \to \sin mp\theta\,\eta(\theta)\,\eta(\Omega-\theta), \tag{4.10b}$$

where $\Omega = 2\pi-\beta$ is the exterior wedge angle, and the step function is defined by

$$\eta(x) = \begin{cases} 1, & x>0,\\ 0, & x<0.\end{cases} \tag{4.11}$$

Then we see that

$$\begin{aligned}[\partial_\theta^2+(mp)^2]\cos mp\theta &= \delta'(\theta)-(-1)^m\delta'(\theta-\Omega),\\ [\partial_\theta^2+(mp)^2]\sin mp\theta &= mp[\delta(\theta)-(-1)^m\delta(\theta-\Omega)].\end{aligned} \tag{4.12}$$

From this we can immediately read off the modified scattering matrix for the wedge:

$$\begin{aligned}\tilde{\mathbf{T}}_{\rm wedge}(\mathbf{r},\mathbf{r}') = -\frac{2p}{\pi}{\sum_{m=0}^{\infty}}'\int_{-\infty}^{\infty}\frac{dk}{2\pi}\frac{1}{\zeta^2} \times\Big\{&\mathbf{E}(\mathbf{r},\mathbf{r}')\left[\delta'(\phi-\beta/2)-(-1)^m\delta'(\phi+\beta/2)\right]\\ &\times\cos mp(\phi'-\beta/2)\\ &+mp\mathbf{H}(\mathbf{r},\mathbf{r}')\left[\delta(\phi-\beta/2)-(-1)^m\delta(\phi+\beta/2)\right]\\ &\times\sin mp(\phi'-\beta/2)\Big\}e^{ik(z-z')}\\ \times\frac{1}{\kappa^2\rho^2}&I_{mp}(\kappa\rho_<)K_{mp}(\kappa\rho_>),\end{aligned} \tag{4.13}$$

where we have shifted to the angular variable ϕ measured from the symmetry plane of the wedge, as shown in Fig. 3, ϕ, $\phi'\in[\beta/2,2\pi-\beta/2]$, and the delta functions are understood to be periodically extended, with period 2π.

B. Two-body Calculation

We now want to use this multiple scattering formalism, particularly Eq. (2.16), to reproduce the results found in Ref. [4]. Putting together the scattering matrix for the atom, Eq. (4.7), and that for the wedge, Eq. (4.13), we obtain the following expression for the Casimir-Polder energy,

$$\begin{aligned}E_{aw} = -i\frac{p}{4\pi^3}\,\mathrm{tr}\,\boldsymbol{\alpha}\int\frac{d\zeta dk}{\kappa^2}\int_0^\infty\frac{d\rho'}{\rho'}&\sum_{m=-\infty}^{\infty}\sum_{m'=-\infty}^{\infty}\\ &\times\left[m\mathbf{E}(\mathbf{r},\mathbf{r}'')-m'p\mathbf{H}(\mathbf{r},\mathbf{r}'')\right]e^{im'p(\phi''-\beta/2)}\\ &\times e^{im\phi}\left[e^{-im\beta/2}-(-1)^{m'}e^{im\beta/2}\right]\\ &\times I_m(\kappa\rho_<)K_m(\kappa\rho_>)I_{|m'|p}(\kappa\tilde{\rho}_<)K_{|m'|p}(\kappa\tilde{\rho}_>).\end{aligned} \tag{4.14}$$

Here $\rho_{<,>}$ is the lesser, greater of ρ,ρ', and $\tilde{\rho}_{<,>}$ is the lesser, greater of ρ'',ρ'. After the differentiations contained in $\mathbf{E}$ and $\mathbf{H}$ are performed, the coordinates ρ'' and ϕ'' are to be set equal to ρ and ϕ, respectively.

Although we can carry out the m summation, or the ρ' integration, it seems difficult to bring Eq. (4.14) into the closed form given in Ref. [4]. So we initially will content ourselves with a special case, $\beta=\pi$ or $p=1$, that is, the interaction of an atom with an infinite conducting plane. In that case, we may as well ultimately set $\phi=\phi''=\pi$. Then only Bessel functions of integer order occur, and both the m and m' sums can be carried out, using the addition theorem,

$$K_0(\kappa P) = \sum_{m=-\infty}^{\infty}e^{im(\phi-\phi')}I_m(\kappa\rho_<)K_m(\kappa\rho_>), \tag{4.15}$$

where

$$P = \sqrt{\rho^2 + \rho'^2 - 2\rho\rho'\cos(\phi - \phi')}. \tag{4.16}$$

Then the energy can be written as

$$\begin{aligned} E_{ap} &= -\frac{i}{2\pi^2}\int_0^\infty \frac{d\kappa}{\kappa}\int_0^\infty \frac{d\rho'}{\rho'}\mathrm{tr}\,\boldsymbol{\alpha}(\mathbf{E}-\mathbf{H})(\mathbf{r},\mathbf{r}'') \\ &\quad\times\Bigg[K_0(\kappa\sqrt{\rho^2+\rho'^2-2\rho\rho'\sin\phi}) \\ &\quad\times\frac{1}{i}\frac{\partial}{\partial\phi''}K_0(\kappa\sqrt{\rho''^2+\rho'^2-2\rho''\rho'\sin\phi''}) \\ &\quad-(\sin\phi\to-\sin\phi)\Bigg]\Bigg|_{\rho''\to\rho,\,\phi''\to\phi=\pi} \\ &= \frac{1}{2\pi^2}\int_0^\infty d\kappa\int_0^\infty d\rho\,\mathrm{tr}\,\boldsymbol{\alpha}(\mathbf{E}-\mathbf{H})(\mathbf{r},\mathbf{r}'') \\ &\quad\times\Bigg[\frac{\rho''\cos\phi''}{\sqrt{\rho'^2+\rho''^2-2\rho'\rho''\sin\phi''}} \\ &\quad\times K_0'(\kappa(\sqrt{\rho'^2+\rho''^2-2\rho'\rho''\sin\phi''}) \\ &\quad\times K_0(\kappa\sqrt{\rho^2+\rho'^2-2\rho\rho'\sin\phi}) \\ &\quad+(\sin\phi\to-\sin\phi)\Bigg]\Bigg|_{\rho''\to\rho,\phi''\to\phi=\pi}. \end{aligned} \tag{4.17}$$

The simplest situation occurs when the atom is only polarizable along the axis of the wedge, $\boldsymbol{\alpha} = \hat{\mathbf{z}}\hat{\mathbf{z}}\alpha_{zz}$. Then $\mathrm{tr}\,\boldsymbol{\alpha}\mathbf{E} = 0$, $\mathrm{tr}\,\boldsymbol{\alpha}\mathbf{H} = \kappa^4\alpha_{zz}$, and we have

$$\begin{aligned} E_{ap} &= -\frac{\alpha_{zz}}{\pi^2}\int_0^\infty d\rho'\frac{\rho}{\sqrt{\rho^2+\rho'^2}}\int_0^\infty d\kappa\,\kappa^4 \\ &\quad\times K_0(\kappa\sqrt{\rho^2+\rho'^2})K_1(\kappa\sqrt{\rho^2+\rho'^2}) \\ &= -\frac{\alpha_{zz}}{8\pi\rho^4}, \end{aligned} \tag{4.18}$$

which is the expected Casimir-Polder energy. With only a bit more effort, we find the familiar result for arbitrary polarization,

$$E_{\mathrm{CP}} = -\frac{\mathrm{tr}\,\boldsymbol{\alpha}}{8\pi\rho^4}. \tag{4.19}$$

Given the difficulty of even analytically reproducing the two-body correction given in Ref. [4], it is not surprising that we did not get very far with the three-body calculation. In the Appendix we consider the scalar analog for the two-body effect, and although we get a bit further, we have been unable to reproduce the analytic result obtained by the direct calculation.[3] So we turn, instead, to another problem, the interaction between an atom and a pair of cylinders.

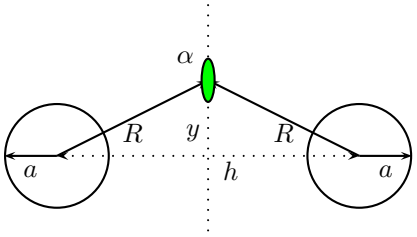

FIG. 4: (Color online) An anisotropically polarizable atom, denoted by α, is symmetrically located relative to two identical parallel perfectly conducting cylinders (with axes coming out of the page). The centers of the cylinders are separated by a distance h, and each has radius a. The atom is on the line bisecting the line connecting the centers of the two cylinders, but a distance y above it. The atom is a distance R from the center of either cylinder. The angle θ is defined by $\cos\theta = y/R$.

V. CASIMIR-POLDER INTERACTION OF ATOM WITH TWO PARALLEL CYLINDERS

The difficulties in extracting usable expressions for three-body effects for the atom-wedge-wedge problem has to do with the lack of a scale, so multipole expansions, for example, are not applicable. Therefore, we turn to another example, that of an atom interacting with a pair of parallel cylinders, illustrated in Fig. 4. Here it is assumed the two cylinders are identical, with radius a, and their centers are separated by a distance h. The atom is located on the line bisecting the line connecting the centers of the cylinders, a distance R from the center of each, and a height y above the centerline. We will consider the case when the atom is only polarizable along the bisecting line.

A. Scattering matrix for cylinder

We first need to compute the scattering matrix for the cylinder. The Green's dyadic, given in Ref. [32], part of which appears in Ref. [5], can be written, with slight notational changes, as[4]

$$\begin{aligned} \boldsymbol{\Gamma}_{\mathrm{cyl}}(\mathbf{r},\mathbf{r}') &= -\sum_{m=-\infty}^{\infty}\int\frac{dk}{(2\pi)^2}e^{im(\phi-\phi')}e^{ik(z-z')} \\ &\quad\times\left[\mathbf{E}F_m(\rho,\rho')+\mathbf{H}G_m(\rho,\rho')\right], \end{aligned} \tag{5.1}$$

[3] However, it is possible to recast the $\tilde{T}_1\tilde{T}_2$ expression into the form of the direct CP energy $E_{CP} = \mathrm{Tr}\int d\zeta\alpha(G-G_0)$—see the Appendix.

[4] As noted in Ref. [33], only the terms in the Green's functions involving modified Bessel functions, and not powers of the radial coordinates, contribute to the electric and magnetic fields.

where the TE and TM Green's functions are, outside the cylinder,

$$F_m(\rho,\rho') = \frac{1}{\kappa^2}\Big[I_m(\kappa\rho_<)K_m(\kappa\rho_>) - \frac{I_m'(\kappa a)}{K_m'(\kappa a)}K_m(\kappa\rho)K_m(\kappa\rho')\Big], \quad (5.2a)$$

$$G_m(\rho,\rho') = \frac{1}{\kappa^2}\Big[I_m(\kappa\rho_<)K_m(\kappa\rho_>) - \frac{I_m(\kappa a)}{K_m(\kappa a)}K_m(\kappa\rho)K_m(\kappa\rho')\Big], \quad (5.2b)$$

and the polarization operators are the same as given in Eqs. (4.2). The modified scattering matrix is given by Eq. (4.8), where, because of the tranversality of the polarization operators, the inverse free Green's operator may be replaced by $\mathbf{\Gamma}_0^{-1} \to \frac{1}{\zeta^2}(\nabla^2 - \zeta^2)$ [cf. Eq. (4.9)], which vanishes everywhere but on the surface of the cylinder. Because we have a perfectly conducting body, $F_m(\rho,\rho') = 0$ if $\rho' > a > \rho$, and so for the TE function with $\rho' > a$

$$(F_m - F_m^0)(\rho,\rho') = -\frac{1}{\kappa^2}K_m(\kappa\rho')\Big[\frac{I_m'(\kappa a)}{K_m'(\kappa a)} \times K_m(\kappa\rho)\eta(\rho-a) + I_m(\kappa\rho)\eta(a-\rho)\Big]. \quad (5.3a)$$

Similarly, the TM functions are

$$(G_m - G_m^0)(\rho,\rho') = -\frac{1}{\kappa^2}K_m(\kappa\rho')\Big[\frac{I_m(\kappa a)}{K_m(\kappa a)} \times K_m(\kappa\rho)\eta(\rho-a) + I_m(\kappa\rho)\eta(a-\rho)\Big]. \quad (5.3b)$$

Then a simple calculation leads to the scattering matrix

$$\tilde{\mathbf{T}}_{\rm cyl} = \sum_{m=-\infty}^{\infty}\int\frac{dk}{(2\pi)^2}e^{ik(z-z')}e^{im(\phi-\phi')}\frac{1}{\kappa^2\zeta^2 a} \times\Big[\mathbf{E}\frac{1}{\kappa}\frac{1}{\rho}\frac{\partial}{\partial\rho}\rho\delta(\rho-a)\frac{K_m(\kappa\rho')}{K_m'(\kappa a)} - \mathbf{H}\delta(\rho-a)\frac{K_m(\kappa\rho')}{K_m(\kappa a)}\Big]. \quad (5.4)$$

To check its validity, we reproduce the two-body interaction between one cylinder and the anisotropic atom, for which we obtain

$$E_{12} = -\frac{1}{2}\int_{-\infty}^{\infty}\frac{d\zeta}{2\pi}\,{\rm Tr}\,\tilde{\mathbf{T}}_{\rm atom}\tilde{\mathbf{T}}_{\rm cyl} = -\int\frac{d\zeta dk}{(2\pi)^2}\sum_{m=-\infty}^{\infty}{\rm tr}\,\frac{\boldsymbol{\alpha}}{\kappa^2}\Big[\frac{I_m'(\kappa a)}{K_m'(\kappa a)}\mathbf{E}(\mathbf{r},\mathbf{r}') + \frac{I_m(\kappa a)}{K_m(\kappa a)}\mathbf{H}(\mathbf{r},\mathbf{r}')\Big] \times K_m(\kappa\rho)K_m(\kappa\rho')\Big|_{\mathbf{r}=\mathbf{r}'=\mathbf{R}}. \quad (5.5)$$

This is the general result, which may be derived by simpler means. In particular, for the situation envisaged in Fig. 4, where $R = h/(2\sin\theta)$, and the atom is only polarizable along the y direction, we obtain the formulas given in Ref. [5][5] in terms of the distance of closest approach $R_0 = h/2$,

$$E_{\rm CP}^{\rm TM} = -\frac{\alpha}{4\pi}\frac{\sin^4\theta}{R_0^4}\sum_{m=-\infty}^{\infty}\int_0^\infty dx\,x\frac{I_m(\kappa a\sin\theta/R_0)}{K_m(\kappa a\sin\theta/R_0)} \times\left[m^2K_m^2(x)\sin^2\theta + x^2K_m'^2(x)\cos^2\theta\right], \quad (5.6a)$$

$$E_{\rm CP}^{\rm TE} = \frac{\alpha}{4\pi}\frac{\sin^4\theta}{R_0^4}\sum_{m=-\infty}^{\infty}\int_0^\infty dx\,x\frac{I_m'(\kappa a\sin\theta/R_0)}{K_m'(\kappa a\sin\theta/R_0)} \times\left[m^2K_m^2(x)\cos^2\theta + x^2K_m'^2(x)\sin^2\theta\right]. \quad (5.6b)$$

These formulas show that repulsion indeed occurs along the bisector (y) direction provided the distance of closest approach R_0 is larger than about 7 times the radius of the cylinder; in this case the $m = 0$ term dominates, and the TM contribution is much larger than the always attractive TE contribution, as we will see below.

B. Three-body correction

We now want to see if the above repulsive effect survives when the effect of both bodies are included. By virtue of the symmetry seen in Fig. 4, the two-body forces in the y-direction are doubled. That is, if the atom is called body 1, and the cylinders are 2 and 3, respectively, the two-body terms are just

$$E_{2-{\rm body}} = E_{12} + E_{13}. \quad (5.7)$$

The three-body terms are computed from Eq. (3.20). In view of the remarks above, because we are considering large distances between the cylinders, it should suffice to consider the three- and four-scattering terms, the higher terms being suppressed,

$$E_{3-{\rm body}} \approx E_{123} + E_{132} + E_{1232} + E_{1323},$$
$$E_{123} = -\frac{1}{2}\,{\rm Tr}\,\tilde{\mathbf{T}}_1\tilde{\mathbf{T}}_2\tilde{\mathbf{T}}_3, \quad E_{1232} = -\frac{1}{2}\,{\rm Tr}\,\tilde{\mathbf{T}}_1\tilde{\mathbf{T}}_2\tilde{\mathbf{T}}_3\tilde{\mathbf{T}}_2. \quad (5.8)$$

Further, we expect dominance by the $m = 0$ TM mode. However, we can effect considerable simplification before we make that last approximation. Indeed, the formula

[5] The signs of the energies given there, and in Fig. 3 of that reference, should be reversed. All physical conclusions in that paper, however, are correct.

for the TM mode 3-scattering energy simplifies to

$$E_{123}^{\rm TM} = \int \frac{d\zeta\, dk}{(2\pi)^2}\frac{1}{\kappa^2}\,{\rm tr}\,\boldsymbol{\alpha}\mathbf{H}(\mathbf{r},\tilde{\mathbf{r}}) \times \sum_{mm'}\int_0^{2\pi}\frac{d\tilde{\phi}'}{2\pi}e^{i(m\phi-m'\tilde{\phi})}e^{i(m'\tilde{\phi}'-m\phi')} \times \frac{I_m(\kappa a)}{K_m(\kappa a)}\frac{K_m(\kappa\rho')}{K_{m'}(\kappa a)}K_m(\kappa\rho)K_{m'}(\kappa\tilde{\rho})\Big|_{\rho=\tilde{\rho}=R}, \tag{5.9}$$

and the corresponding TE 3-scattering energy is

$$E_{123}^{\rm TE} = \int \frac{d\zeta\, dk}{(2\pi)^2}\frac{1}{\kappa^2}\,{\rm tr}\,\boldsymbol{\alpha}\mathbf{E}(\mathbf{r},\tilde{\mathbf{r}}) \times \sum_{mm'}\int_0^{2\pi}\frac{d\tilde{\phi}'}{2\pi}e^{i(m\phi-m'\tilde{\phi})}e^{i(m'\tilde{\phi}'-m\phi')} \times \frac{I'_m(\kappa a)}{K'_m(\kappa a)}\frac{K'_m(\kappa\rho')}{K'_{m'}(\kappa a)}\frac{d\rho'}{da}K_m(\kappa\rho)K_{m'}(\kappa\tilde{\rho})\Big|_{\rho=\tilde{\rho}=R}, \tag{5.10}$$

where a and $\tilde{\phi}'$ are the cylindrical coordinates of a point on the surface of the second cylinder relative to the central axis of that cylinder, the same point being located at cylindrical coordinates ρ' and ϕ' relative to the central axis of the first cylinder. These coordinates are related by

$$\rho'^2 = h^2+a^2-2ah\cos\tilde{\phi}', \quad \tan\phi' = \frac{a\sin\tilde{\phi}'}{a\cos\tilde{\phi}'-h}. \tag{5.11}$$

The atom is located in the two coordinate systems at

$$\mathbf{R} = (R,\phi,0) = (R,\tilde{\phi},0), \tag{5.12}$$

where

$$\phi = \frac{\pi}{2}+\theta, \quad \tilde{\phi} = \frac{\pi}{2}-\theta. \tag{5.13}$$

It would now be straightforward to work out the multipole expansion of Eqs. (5.9), (5.10) that is, a power series expansion in powers of a/h. We will content ourselves with the lowest term, which means we can set $m = 0$, because only for small values of a/h do we have 2-body repulsion. Higher terms are suppressed by powers of a/h. In this limit, the TE energy is completely negligible, because of the appearance of derivatives of Bessel functions. The behavior of the Bessel functions for small argument makes this point clear:

$$I_0(z) \sim 1+\frac{1}{4}z^2, \quad K_0(z) \sim -\gamma-\ln\frac{z}{2}, \tag{5.14a}$$

$$I'_0(z) \sim \frac{1}{2}z, \quad K'_0(z) \sim -\frac{1}{z}, \quad z\to 0. \tag{5.14b}$$

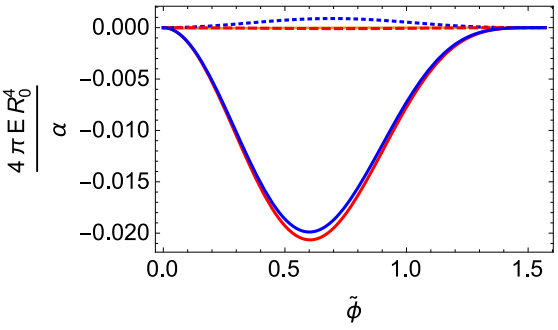

FIG. 5: (Color online) The Casimir-Polder energy of an anisotropic atom or nanoparticle passing on the symmetry line perpendicular to a pair of identical perfectly conducting parallel cylinders. The energy, apart from a factor of $\alpha/(4\pi R_0^4)$, is plotted versus $\tilde{\phi} = \pi/2-\theta$, that is, the angle between the line connecting the axes of the cylinders and the line connecting the atom with the center of either cylinder. The bottom curve (red) is the two-body energy, the top curve (dotted-blue) is the three-scattering correction, the second-from-top curve (dashed red) is the four-scattering term, while the second curve from the bottom (blue) is the total Casimir-Polder energy. The energies are plotted for $a/R_0 = 0.01$. Because $a/R_0 \ll 1$ it is sufficient to include only $m = 0$ for the three-body corrections. Also, the TE contributions are completely negligible. It is seen that the three-body effects, in fact, are very small, and do not significantly alter the repulsion between the atom and the pair of cylinders, and the four-scattering terms are quite negligible.

Then we get a very simple explicit formula, again for an atom polarizable only in the bisector (y) direction,

$$E_{123}^{\rm TM} \sim \frac{\alpha_{yy}}{4\pi R_0^4}\cos^2\theta\sin^4\theta \times \int_0^\infty dx\, x^3\frac{K_0(2x\sin\theta)I_0(xa\sin\theta/R_0)}{K_0^2(xa\sin\theta/R_0)}K_0'^2(x). \tag{5.15}$$

Here $h = 2R_0$ is the separation distance between the axes of the cylinders. In the same approximation, the 4-scattering contribution is also given simply:

$$E_{1232}^{\rm TM} \sim -\frac{\alpha_{yy}}{4\pi R_0^4}\cos^2\theta\sin^4\theta \times \int_0^\infty dx\, x^3\frac{K_0^2(2x\sin\theta)I_0(xa\sin\theta/R_0)}{K_0^3(xa\sin\theta/R_0)}K_0'^2(x). \tag{5.16}$$

These TM corrections are plotted in Fig. 5 as a function of $\tilde{\phi} = \pi/2-\theta$, so $\tilde{\phi} = 0$ at the position of the atom closest to the cylinders, and compared to the two body contributions. (All the TE corrections are completely negligible.) The figure shows the two-body CP energy, entirely dominated by the $m = 0$ TM contribution, and the $m = 0$ three-body correction, dominated by the three-scattering terms, in the limit of large distance between the cylinders. The TE contributions were com-

puted, but found, as expected, to be completely insignificant in the large distance regime. The TM three-body correction is not quite negligible, but does not affect the Casimir-Polder repulsion discovered in Ref. [5].

VI. DIFFICULTY OF ACHIEVING HIGH ATOMIC ANISOTROPY

In order for Casimir–Polder repulsion to be possible, the atom interacting with a body must have a sufficiently anisotropic polarizability tensor. Defining an anisotropy factor γ according to

$$\boldsymbol{\alpha} = \alpha_{zz}\hat{\mathbf{z}}\hat{\mathbf{z}} + \gamma\alpha_{zz}\hat{\mathbf{x}}\hat{\mathbf{x}} + \gamma\alpha_{zz}\hat{\mathbf{y}}\hat{\mathbf{y}}, \tag{6.1}$$

implying

$$\gamma = \frac{\mathrm{Tr}(\boldsymbol{\alpha}) - \alpha_{zz}}{2\alpha_{zz}}, \tag{6.2}$$

we found in Ref. [4] that for an anisotropic atom interacting with a half-plane, the critical value of γ was 1/4. Values $\gamma < 1/4$ give repulsion in certain circumstances, whereas for $\gamma > 1/4$ no repulsion is possible. The non-retarded interaction of an atom and a circular aperture was considered in Ref. [34] and the critical value of γ was found to be 1/4 also in this case [4].

In this section we investigate what minimal value of the anisotropy parameter can be achieved by preparing an atom in an excited eigenstate $|nlm\rangle$. Here, n denotes the principal quantum number, $l = 0, \ldots n-1$ is the quantum number for the orbital angular momentum and $m = -l \ldots l$ that for its z-component. The question is of great interest especially in the light of recent advances in experimental techniques using Rydberg atoms, atoms excited to high principal quantum numbers, near boundaries [35, 36], and noting that Rydberg atoms can take highly anisotropic shapes.

Because of the close spacing of energy levels for highly excited states, and the fact that transitions to the states nearest in energy to $|nlm\rangle$ dominate the CP energy [36], the Casimir–Polder interaction of a Rydberg molecule is essentially non-retarded even at atomically large separations, up to hundreds of micrometers. It was shown that in such cases the interaction energy is proportional to the atomic dipole moment tensor [37, 38],

$$E_{nlm} = -\langle \mathbf{dd} \rangle : \boldsymbol{\nabla}\boldsymbol{\nabla} G\Big|_{\omega=0} = -\langle \mathbf{dd} \rangle : \boldsymbol{\Gamma}_{\omega=0}, \tag{6.3}$$

according to Eq. (2.2). For convenience we will work with the ratio

$$q = \langle d_{zz}^2 \rangle / \langle \mathbf{d}^2 \rangle. \tag{6.4}$$

Defining γ similarly as before

$$\gamma = \frac{\langle \mathbf{d}^2 \rangle - \langle d_{zz}^2 \rangle}{2\langle d_{zz}^2 \rangle} = \frac{1}{2}\left(\frac{1}{q} - 1\right), \tag{6.5}$$

we will consider energy eigenstates $|nlm\rangle$ such that anisotropy becomes maximal, i.e., γ becomes minimal and q maximal.

To evaluate the anisotropy parameter, we insert the completeness relation $\sum_{n'l'm'} |n'l'm'\rangle\langle n'l'm'| = I$,

$$q = \frac{\sum_{n'l'm'} \langle nlm|d_z|n'l'm'\rangle\langle n'l'm'|d_z|nlm\rangle}{\sum_{n'l'm'} \langle nlm|\mathbf{d}|n'l'm'\rangle \cdot \langle n'l'm'|\mathbf{d}|nlm\rangle} \tag{6.6}$$

The dipole-matrix elements can conveniently be calculated by means of the Wigner–Eckart theorem [39, 40]

$$\langle n'l'm'|d_s|nlm\rangle = (-1)^{l'-m'} \begin{pmatrix} l' & 1 & l \\ -m' & s & m \end{pmatrix} \langle n'l'||\mathbf{d}||nl\rangle \,, \tag{6.7}$$

where $\langle n'l'||\boldsymbol{d}||nl\rangle$ denotes the reduced matrix element and the Wigner 3-j symbol can be given in terms of Clebsch–Gordan coefficients as [41]

$$\begin{pmatrix} j_1 & j_2 & j \\ m_1 & m_2 & m \end{pmatrix} = \frac{(-1)^{j_1-j_2-m}}{\sqrt{2j+1}} \langle j_1 m_1 j_2 m_2 | j \; -m\rangle \,. \tag{6.8}$$

Substituting these relations into Eq. (6.6) and using the orthonormality relation [41]

$$\sqrt{2j+1} \sum_{m_1 m_2} \begin{pmatrix} j_1 & j_2 & j \\ m_1 & m_2 & m \end{pmatrix} \begin{pmatrix} j_1 & j_2 & j' \\ m_1 & m_2 & m' \end{pmatrix} = \delta_{jj'}\delta_{mm'} \,, \tag{6.9}$$

we find

$$q \to q_{lm} = \sum_{l'} |\langle l\, m\, 1\, 0 | l' m\rangle|^2 \,. \tag{6.10}$$

As expected from the symmetry of the problem, the anisotropy parameter depends neither on the reduced matrix element nor on the principal quantum numbers.

The Clebsch-Gordan coefficients in Eq. (6.10) can be evaluated explicitly, leading to [41]

$$q_{lm} = \frac{l^2 - m^2}{(2l-1)(2l+1)} + \frac{(l+1)^2 - m^2}{(2l+1)(2l+3)} \,. \tag{6.11}$$

For a given l, the anisotropy parameter obviously takes its maximum value for $m = 0$,

$$q_{l0} = \frac{l^2}{(2l-1)(2l+1)} + \frac{(l+1)^2}{(2l+1)(2l+3)} = \frac{2l(l+1)-1}{4l(l+1)-3} \,. \tag{6.12}$$

The latter expression is equal to 1/3 for $l = 0$, approaches 1/2 for $l \to \infty$ and takes it maximum value

$$q_{10} = \tfrac{3}{5} \quad \Longrightarrow \quad \gamma = \tfrac{1}{3} \tag{6.13}$$

for $l = 1$. The maximally anisotropic eigenstate of orbital angular momentum is thus a p state.

Since q_{lm} is positive for any given choice of quantum numbers, it immediately follows that the anisotropy parameter γ is bounded below by 1/3 for any incoherent superposition of energy eigenstates. It is possible that stronger anisotropies could be realizable with a coherent superposition of states. However, the more likely venue for discovering such repulsive effects would be with anisotropic particles, such as elongated needles.

VII. CONCLUSIONS

One of the principal features of Casimir or quantum vacuum forces is that they are not additive. Unlike classical electrodynamics, one cannot simply sum pairwise forces. Such approximations clearly are invalid even for the simplest situations of parallel plates. This, of course, makes calculations more challenging.

In this paper, we have explored some aspects of three-body interactions in the context of Casimir-Polder forces between an anisotropically polarizable atom or nanoparticle and two conducting surfaces. First we examined the role of such forces involving an atom between two perfectly conducting plates, a well-known problem [17], but one in which we can test our formalism and isolate explicitly the three-body terms. Then we turned to the interaction of such an atom with a pair of wedges; we reproduced the repulsive effects seen for an atom interacting with a single wedge [4], but a closed form for the three-body correction remains elusive. So we then examined the interaction of an anisotropic atom with a pair of parallel cylinders. The two-body repulsive effect found earlier [5] was reproduced, and the three-body correction was computed in the limit of large separation between the cylinders, which is the regime where repulsion is expected. The three-body correction is non-negligible in this limit, is completely captured by the TM three-scattering approximation, but is too small to affect the earlier-found repulsion.

Acknowledgments

KAM, EKA, and PP thank the US National Science Foundation, the US Department of Energy, the Simons Foundation, and the Julian Schwinger Foundation for partial support of this research. Some of this work was accomplished while KAM was partially supported by Laboratoire Kastler Brossel, CNRS; he also thanks NTNU for hospitality. We also thank K. V. Shajesh and M. Schaden for useful discussions. SYB gratefully acknowledges support by the German Research Council (grant BU 1803/3-1) and the Freiburg Institute for Advanced Studies.

Appendix: Scalar analog for atom-wedge problem

In this Appendix we will consider a scalar analog of the atom-wedge problem. Let the atom be described by the potential

$$V_{\rm atom} = 4\pi\alpha\delta(\mathbf{r}-\mathbf{R}), \tag{A.1}$$

where $\mathbf{R} = (R,\phi,0)$ is the position of the atom. The modified scattering matrix for the (Dirichlet) wedge is [note that the sign is reversed compared to Eq. (4.8)]

$$\tilde{T}_{\rm wedge} = 1 - G_0^{-1} G_w, \tag{A.2}$$

where

$$G_w(\mathbf{r},\mathbf{r}') = \frac{2p}{\pi}\int_{-\infty}^{\infty}\frac{dk}{2\pi}e^{ik(z-z')}\sum_{m=1}^{\infty}\sin mp(\phi-\beta/2) \times \sin mp(\phi'-\beta/2) I_{mp}(\kappa\rho_<)K_{mp}(\kappa\rho_>). \tag{A.3}$$

Applying $G_0^{-1} = -\nabla^2 + \zeta^2$ we obtain the scattering matrix on the wedge:

$$\tilde{T}_w = \frac{2p}{\pi}\int_{-\infty}^{\infty}\frac{dk}{2\pi}\sum_{m=1}^{\infty}e^{ik(z-z')}\frac{mp}{\rho^2}[\delta(\phi-\beta/2) - (-1)^m\delta(\phi+\beta/2)]\sin mp(\phi'-\beta/2) \times I_{mp}(\kappa\rho_<)K_{mp}(\kappa\rho_>). \tag{A.4}$$

The two-body energy is given by

$$E_{12} = \frac{i}{2}\int\frac{d\omega}{2\pi}\,\mathrm{Tr}\,\tilde{T}_1\tilde{T}_2 = -\frac{1}{2}\int_{-\infty}^{\infty}\frac{d\zeta}{2\pi}\,\mathrm{Tr}\,V_1 G_0 \tilde{T}_2. \tag{A.5}$$

If we use the two-dimensional representation for the free propagator,

$$G_0(\mathbf{r}) = \int_{-\infty}^{\infty}\frac{dk_z}{2\pi}e^{ik_z z}\frac{1}{2\pi}K_0(\kappa|\mathbf{r}_\perp|), \tag{A.6}$$

the two-body energy can be written as

$$E_{12} = -\frac{\alpha}{\pi^2}p^2\int_0^\infty d\kappa\,\kappa\int_0^\infty\frac{d\rho'}{\rho'}\sum_{m=1}^{\infty}m\sin mp(\phi-\beta/2) \times I_{mp}(\kappa\rho_<)K_{mp}(\kappa\rho_>) \times[K_0(\kappa P_+) - (-1)^m K_0(\kappa P_-)], \tag{A.7}$$

where $P_\pm$ is the distance between the atom and a point on the upper (lower) wedge boundary,

$$P_\pm = \sqrt{R^2+\rho'^2 - 2R\rho'\cos(\phi\mp\beta/2)}. \tag{A.8}$$

Now the integral of the three Bessel functions can be performed:

$$\int_0^\infty dt\,t\,I_\nu(\xi t)K_\nu(t)K_0(P_\pm t/\rho_>) = \frac{1}{2\xi\sin(\phi-\beta/2)}\sum_{n=0}^{\infty}\xi^{\nu+n+1}\frac{\sin(n+1)(\phi-\beta/2)}{\nu+n+1}, \tag{A.9}$$

where $\xi = \rho_</\rho_>$. The radial integrals are then easy, and we are immediately led to

$$E_{12} = -\frac{\alpha p^2}{\pi^2 R^2}\sum_{m=1}^{\infty}m\sin mp(\phi-\beta/2) \times\sum_{n=0}^{\infty}\frac{1}{(n+mp)(n+mp+2)} \times\left[\frac{\sin(n+1)(\phi-\beta/2)}{\sin(\phi-\beta/2)} - (-1)^m\frac{\sin(n+1)(\phi+\beta/2)}{\sin(\phi+\beta/2)}\right]. \tag{A.10}$$

Now we replace the sum over m by an integral,

$$\sum_{m=1}^{\infty} \frac{1}{mp+N} e^{imp\theta} = \sum_{m=1}^{\infty} \int_0^\infty dt\, e^{-t(mp+N)} e^{imp\theta} = \int_0^\infty dt\, e^{-tN} \frac{1}{e^{p(t-i\theta)}-1}. \quad \text{(A.11)}$$

Then the n sum can be carried out as a geometric series, and the result is a single integral,

$$E_{12} = -\frac{\alpha p^2}{4\pi^2 R^2} \int_0^\infty dt \sinh t \sinh pt \sin(\phi-\beta/2) \times \left\{ \frac{1}{[\cosh pt - \cos p(\phi-\beta/2)]^2} \frac{1}{\cosh t - \cos(\phi-\beta/2)} + \frac{1}{[\cosh pt + \cos p(\phi-\beta/2)]^2} \frac{1}{\cosh t - \cos(\phi+\beta/2)} \right\}. \quad \text{(A.12)}$$

Alternatively, we can directly calculate the two-body energy from

$$E_{12} = \frac{1}{2} \int_{-\infty}^{\infty} \frac{d\zeta}{2\pi} V_1 (G - G_0). \quad \text{(A.13)}$$

which may be directly evaluated in closed form:

$$E_{12} = -\frac{\alpha}{8\pi R^2} \left[\frac{p^2}{\sin^2 p(\phi-\beta/2)} + \frac{1}{3}(1-p^2) \right]. \quad \text{(A.14)}$$

The form (A.12) may be evaluated straightforwardly in analytic form for the two special cases $p = 1$ ($\beta = \pi$, that is, a plane), and $p = 1/2$ ($\beta = 0$, that is, a half-plane), in agreement with Eq. (A.14),

$$E_{12}(p=1) = -\frac{\alpha}{8\pi R^2} \frac{1}{\sin^2\theta}, \quad \text{(A.15a)}$$

$$E_{12}(p=1/2) = -\frac{\alpha}{32\pi R^2} \left(\frac{1}{\sin^2 \theta/2} + 1 \right) \quad \text{(A.15b)}$$

For other values of p the analytic evaluation of Eq. (A.12) seems nontrivial; however, the integral is rapidly convergent, and the numerical coincidence with the closed form (A.14) is easily verified.

Not surprisingly, it is possible to show that the explicit form of Eq. (A.13) follows from the multiple scattering form of the two-body energy (A.7), written in terms of a sum over four Bessel functions and a sum over m and m' as in Eq. (4.14). This involves using the integral [notation as in Eq. (4.14), with $\nu = m'p$],

$$\int \frac{d\rho'}{\rho'} I_m(\kappa\rho_<) K_m(\kappa\rho_>) I_\nu(\kappa\tilde{\rho}_<) K_\nu(\kappa\tilde{\rho}_>) = \frac{1}{m^2-\nu^2} [K_\nu(\kappa R) I_\nu(\kappa R) - I_m(\kappa R) K_m(\kappa R)], \quad \text{(A.16)}$$

where the resulting two terms in the energy are summed over m and m', respectively, using

$$\sum_{m=-\infty}^{\infty} \frac{e^{im\theta}}{m^2-\nu^2} = -\frac{\pi}{\nu} \frac{\cos\nu(\theta-\pi)}{\sin\pi\nu}, \quad \text{(A.17a)}$$

$$\sum_{m'=1}^{\infty} \frac{m'p \sin m'p}{m^2-(m'p)^2} = -\frac{\pi}{2p} \sin\frac{m}{p}(\pi - p\theta) \csc\frac{m\pi}{p}, \quad \text{(A.17b)}$$

$$\sum_{m'=1}^{\infty} (-1)^{m'} \frac{m'p \sin m'p}{m^2-(m'p)^2} = -\frac{\pi}{2p} \sin m\theta \csc\frac{m\pi}{p}. \quad \text{(A.17c)}$$

[1] H. B. G. Casimir, "On the Attraction Between Two Perfectly Conducting Plates," Kon. Ned. Akad. Wetensch. Proc. **51**, 793 (1948).

[2] *Lecture Notes in Physics: Casimir physics*, eds. Diego Dalvit, Peter Milonni, David Roberts, and Felipe da Rosa (Springer, 2011), vol. **834**, (2011).

[3] M. Levin, A. P. McCauley, A. W. Rodriguez, M. T. H. Reid, and S. G. Johnson, "Casimir Repulsion between Metallic Objects in Vacuum," Phys. Rev. Lett. **105**, 090403 (2010).

[4] K. A. Milton, E. K. Abalo, P. Parashar, N. Pourtolami, I. Brevik, and S. A. Ellingsen, "Casimir-Polder repulsion near edges: wedge apex and a screen with an aperture," Phys. Rev. A **83**, 062507 (2011) [arXiv:1103.4386 [hep-th]].

[5] K. A. Milton, P. Parashar, N. Pourtolami, and I. Brevik, "Casimir-Polder repulsion: Polarizable atoms, cylinders, spheres, and ellipsoids," Phys. Rev. D **85**, 025008 (2012) [arXiv:1111.4224 [hep-th]].

[6] K. V. Shajesh and M. Schaden, "Repulsive long-range forces between anisotropic atoms and dielectrics," Phys. Rev. A **85**, 012523 (2012) [arXiv:1112.1348 [physics.atom-ph]].

[7] K. A. Milton, E. K. Abalo, P. Parashar, N. Pourtolami, I. Brevik, and S. A. Ellingsen, "Repulsive Casimir and Casimir-Polder Forces," J. Phys. A **45**, 374006 (2012) [arXiv:1202.6415 [hep-th]].

[8] M. Boström, S. Å. Ellingsen, I. Brevik, M. F. Dou, C. Persson, and Bo E. Sernelius, "Casimir attractive-repulsive transition in MEMS," Eur. Phys. J. B **85**, 377 (2012).

[9] M. Boström, B. W. Ninham, I. Brevik, C. Persson, D. F. Parsons, and Bo E. Sernelius, "Ultrathin metallic coatings can induce quantum levitation between nanosurfaces," Appl. Phys. Lett. **100**, 253104 (2012). [Erratum: Appl. Phys. Lett. **103**, 039902 (2013).]

[10] M. Dou, F. Lou, M. Boström, I. Brevik, and C. Persson, "Casimir quantum levitation tuned by means of material properties and geometries," Phys. Rev. B **89**, 201407(R) (2014).

[11] T. Emig, N. Graham, R. L. Jaffe and M. Kardar, "Casimir Forces between Compact Objects. I. The Scalar Case," Phys. Rev. D **77**, 025005 (2008) [arXiv:0710.3084 [cond-mat.stat-mech]].

[12] M. Schaden, "Irreducible Many-Body Casimir Energies of Intersecting Objects," Europhys. Lett. **94**, 41001 (2011) [arXiv:1011.2475 [quant-ph]].

[13] K. V. Shajesh and M. Schaden, "Many-Body Contributions to Green's Functions and Casimir Energies," Phys. Rev. D **83**, 125032 (2011) [arXiv:1103.3048 [hep-th]].

[14] J. Schwinger, L. L. DeRaad, Jr., and K. A. Milton, "Casimir Effect in Dielectrics," Ann. Phys. (N.Y.) **115**, 1 (1979).

[15] K. A. Milton, L. L. DeRaad, Jr., and J. Schwinger, "Casimir Selfstress on a Perfectly Conducting Spherical Shell," Ann. Phys. (N.Y.) **115**, 388 (1978).

[16] J. Schwinger, "Casimir Effect in Source Theory," Lett. Math. Phys. **1**, 43 (1975).

[17] G. Barton, "Quantum Electrodynamic Level Shifts Between Parallel Mirrors: Analysis," Proc. Roy. Soc. Lond. A **410**, 141 (1987).

[18] K. A. Milton, E. Abalo, P. Parashar, and K. V. Shajesh, "Three-body Casimir-Polder interactions," Nuovo Cim. C **036**, 183 (2013) [arXiv:1301.2484 [quant-ph]].

[19] S. Zaheer, A. W. Rodriguez, S. G. Johnson, and R. L. Jaffe, "Optical-approximation analysis of sidewall-spacing effects on the force between two squares with parallel sidewalls," Phys. Rev. A **76**, 063816 (2007) [arXiv:0709.0699 [quant-ph]].

[20] A. Rodriguez, M. Ibanescu, D. Iannuzzi, F. Capasso, J. D. Joannopoulos, and S. G. Johnson, "Computation and visualization of Casimir forces in arbitrary geometries: non-monotonic lateral forces and failure of proximity-force approximations," Phys. Rev. Lett. **99**, 080401 (2007).

[21] P. Rodriguez-Lopez, S. J. Rahi, and T. Emig, "Three-body Casimir effects and non-monotonic forces," Phys. Rev. A **80** 022519 (2009).

[22] K. A. Milton, R. Guérout, G. L. Ingold, A. Lambrecht, and S. Reynaud, "Negative Casimir Entropies in Nanoparticle Interactions," arXiv:1405.0311 [quant-ph], to appear in special issue on Casimir Physics in J. Phys. Cond. Mat.

[23] K. A. Milton, P. Parashar, E. K. Abalo, F. Kheirandish, and K. Kirsten, "Investigations of the torque anomaly in the annular sector. II. Global calculations, electromagnetic case," Phys. Rev. D **88**, 045030 (2013) [arXiv:1307.2535 [hep-th]].

[24] R. Guérout, A. Lambrecht, K. A. Milton, and S. Reynaud, "Derivation of the Lifshitz-Matsubara sum formula for the Casimir pressure between metallic plane mirrors," Phys. Rev. E **90**, 042125 (2014).

[25] P. R. Berman, G. W. Ford, and P. W. Milonni, "Coupled-oscillator theory of dispersion and Casimir-Polder interactions," J. Chem. Phys. **141**, 164105 (2014).

[26] H. Alnes, K. Olaussen, F. Ravndal, and I. K. Wehus, "Resolution of an apparent inconsistency in the electromagnetic Casimir effect," J. Phys. A: Math. Gen. **40**, F315 (2007).

[27] H. Alnes, F. Ravndal, I. K. Wehus, and K. Olaussen, "Electromagnetic Casimir energy with extra dimension," Phys. Rev. D **74**, 105017 (2006).

[28] I. Brevik and K. A. Milton, "Casimir energies: Temperature dependence, dispersion, and anomalies," Phys. Rev. E **78**, 011124 (2008).

[29] X. Li, X. Shi, and J. Zhang, "Generalized Riemann ζ-function regularization and Casimir energy for a piecewise uniform string," Phys. Rev. D **44**, 560 (1991).

[30] I. Brevik, "Casimir theory of the relativistic composite string revisited, and a formally related problem in scalar QFT," J. Phys. A: Math. Theor. **45**, 374003 (2012).

[31] I. Brevik, A. A. Bytsenko, and B. M. Pimentel, "Thermodynamic properties of the relativistic composite string—Expository remarks," In Theoretical Physics 2002, Part 2, editors T. F. George and H. F. Arnoldus (Nova Sci. Publ., New York 2003), p. 117 [arXiv hep-th/0108116]].

[32] L. L. DeRaad, Jr. and K. A. Milton, "Casimir Selfstress On A Perfectly Conducting Cylindrical Shell," Ann. Phys. (N.Y.) **136**, 229 (1981).

[33] I. Cavero-Pelaez and K. A. Milton, Ann. Phys. (N.Y.) **320**, 108 (2005) [hep-th/0412135].

[34] C. Eberlein and R. Zietal, "Casimir-Polder interaction between a polarizable particle and a plate with a hole," Phys. Rev. A **83**, 052514 (2011).

[35] H. Kübler, J. P. Schaffer, T. Baluktsian, R. Löw, and T. Pfau, "Coherent Excitation of Rydberg Atoms in Thermal Vapor Microcells," Nature Photonics **4**, 112 (2010).

[36] J. A. Crosse, S. Å. Ellingsen, K. Clements, S. Y. Buhmann, and S. Scheel, "Thermal Casimir-Polder shifts in Rydberg atoms near metallic surfaces," Phys. Rev. A **82**, 010901(R) (2010).

[37] S. Å. Ellingsen, S. Y. Buhmann, and S. Scheel, Phys. "Temperature-invariant Casimir-Polder forces despite large thermal photon numbers," Rev. Lett. **104**, 223003 (2010).

[38] S. Å. Ellingsen, S. Y. Buhmann, and S. Scheel, "Temperature-independent Casimir-Polder forces in arbitrary geometries," Phys. Rev. A **84**, 060501(R) (2011).

[39] E. Wigner, "Einige Folgerungen aus der Schrödingerschen Theorie für die Termstrukturen," Z. Phys. **43**, 624 (1927).

[40] C. Eckart, "The Application of Group Theory to the Quantum Dynamics of Monatomic Systems," Rev. Mod. Phys. **2**, 305 (1930).

[41] A. R. Edmonds, *Angular Momentum in Quantum Mechanics* (Princeton University Press, Princeton, New Jersey, 1996).